JOSEPHSON QUANTUM BITS IN THE FLUX REGIME

Yuriy Makhlin[a b], Gerd Schön[a c], and Alexander Shnirman[a].

[a]Institut für Theoretische Festkörperphysik, Universität Karlsruhe, D-76128 Karlsruhe, Germany

[b]Landau Institute for Theoretical Physics, Kosygin St. 2, 117940, Moscow, Russia

[c]Forschungszentrum Karlsruhe, Institut für Nanotechnologie, D-76021 Karlsruhe

Josephson junction circuits can serve as building blocks of quantum computers. Here we discuss designs, which employ magnetic flux degrees of freedom to process quantum information. Elementary single-qubit and two-qubit logic gates can be performed by voltage or current pulses. The coherence time should be long enough to allow a series of such operations. We also discuss the readout, i.e. a quantum measurement process, which is accomplished by coupling a dc-SQUID to the qubit.

1. INTRODUCTION

Josephson junction circuits are particularly suitable for quantum information processing, since they combine the coherence of the superconducting state and the possibility to control the circuit dynamics by voltage and magnetic flux pulses. They can be scaled up to large numbers of qubits and their fabrication and manipulation are possible with present-day technologies. The dynamical variables in these circuits are the phase of the superconducting order parameter and the charge on the junctions. These variables are conjugate and satisfy Heisenberg's uncertainty principle. Depending on the ratio of two characteristic energies — the typical charging energy, which favors well-defined charges, and the Josephson energy, which favors the phase degree of freedom — the charge or the flux can have a well-defined value, while the other fluctuates strongly. Either charge [1–3] or phase [4,5] degrees of freedom can be used to store and process quantum information. Here we describe nano-electronic flux quantum bits and possible designs of the needed circuits.

The qubits form the basic elements of a quantum computer. For single-bit logic gates they should be manipulated, separately for each qubit, by controlling the Hamiltonian. Additionally, to perform two-bit logic operations, one needs to be able to couple qubits in a controlled way. The whole system should stay coherent for a sufficiently long time. This requires that the coupling to the environment is weak. Finally, to read out the information about the state of the system a quantum measurement should be performed. Below we discuss these steps for several designs.

2. JOSEPHSON-JUNCTION FLUX QUBITS

Part of the material presented in the following sections has been described in a review [6]. Here, to make the paper self-contained, we briefly summarize ideas on the design and coherence properties of flux qubits, before presenting new results on the measurement process.

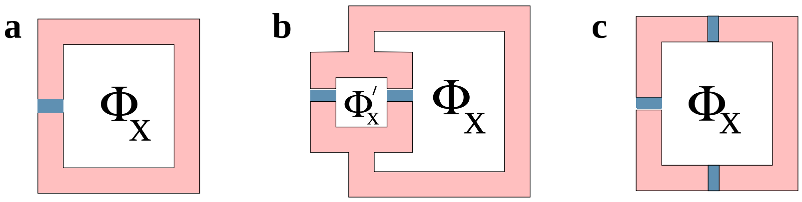

Figure 1. **a**. The rf-SQUID, the simplest flux qubit. **b**. A flux qubit with controlled barrier height between the wells. **c**. A three-junction design.

The simplest design of a controllable two-state quantum system in the limit of dominating Josephson coupling is the rf-SQUID, that is a superconducting loop interrupted by a Josephson junction (see Fig. 1a). The phase difference across the junction, $2\pi\Phi/\Phi_0$, is related to the flux Φ in the loop, which fluctuates around the externally applied value Φ_x. With the Josephson coupling, charging energy and magnetic contributions taken into account, the Hamiltonian of the system reads

$$\mathcal{H} = -E_\mathrm{J}\cos\left(2\pi\frac{\Phi}{\Phi_0}\right) + \frac{(\Phi-\Phi_\mathrm{x})^2}{2L} + \frac{Q^2}{2C_\mathrm{J}}\ . \tag{1}$$

Here L is the self-inductance of the loop and C_J the junction capacitance. The charge $Q = (\hbar/i)\partial/\partial\Phi$ on this capacitor is canonically conjugate to the flux. Under the conditions $\beta_L \equiv 4\pi^2 L E_\mathrm{J}/\Phi_0^2 \geq 1$ and $\Phi_\mathrm{x} \approx \Phi_0/2$ the first two terms of the Hamiltonian define a double-well potential near $\Phi = \Phi_0/2$. At low temperatures the lowest states in the wells dominate the physics of the system with reduced Hamiltonian given by

$$\mathcal{H} = \frac{\varepsilon}{2}\hat{\sigma}_z + \frac{\Delta}{2}\hat{\sigma}_x\ . \tag{2}$$

Here $\varepsilon(\Phi_\mathrm{x}) = 4\pi E_\mathrm{J}\sqrt{6(\beta_L-1)}(\Phi_\mathrm{x}/\Phi_0 - 1/2)$ is the asymmetry of the double well and Δ the tunneling amplitude between the wells. The latter can be controlled via the height of the barrier, which is determined by E_J. This Josephson energy can be manipulated by a separately controlled flux, Φ'_x, if the junction is replaced by a dc-SQUID as shown in Fig. 1b.

The rf-SQUID described above was studied in connection with the concepts of 'macroscopic quantum coherence', that is coherent oscillations of a quantum system between two macroscopically different states [7,8]. However, the requirements of sufficiently large self-inductance and Josephson energy of the junction make the rf-SQUID very susceptible to external noise, and experiments with the rf-SQUID were not successful so far.

To overcome this difficulty Mooij et al. [5] proposed to use a smaller superconducting loop with three junctions (Fig. 1c). In this low-inductance circuit ($L \sim 5$ pH) the flux through the loop remains close to the external bias, $\Phi = \Phi_\mathrm{x}$. Hence the phase differences across the junctions are constrained by $\varphi_1 + \varphi_2 + \varphi_3 = 2\pi\Phi_\mathrm{x}/\Phi_0$, leaving φ_1 and φ_2 as independent dynamical variables. The Josephson couplings produce a potential landscape $U(\varphi_1, \varphi_2)$. Under certain conditions [5,9] a double-well potential is formed within each $2\pi \times 2\pi$ cell in the phase plane. The resulting two lowest states form a two-state quantum system, with different current configurations. Due to the low inductance the system is less affected by the external noise and hence dephasing effects are weak. The Delft group [10] performed microwave spectroscopy experiments on the three-junction system, probing the superpositions of the lowest states in two wells of the Josephson potential landscape. In the spectrum they observed a level repulsion at the degeneracy point, confirming the predictions of the two-state model (2).

The group at Stony Brook [11] probed spectroscopically the superposition of *excited* states in an rf-SQUID. A substantial separation of the minima of the double-well potential (of order Φ_0) and a high barrier made the tunnel coupling between the lowest states in the wells negligible. However, both wells contain a set of higher localized levels. Being closer to the top of the barrier these states mix stronger and form eigenstates, which are superpositions of localized flux states from different wells. The states differ macroscopically: in current by 2–3 μA and in magnetic moment by 10^{10} μ_B.

3. COUPLING OF QUBITS

To perform quantum computation steps, two-bit logic operations in a register of qubits are necessary. For a unitary transformation of the state of two qubits, the couplings between the qubits should be controlled individually for each pair. One way to achieve this is to use a flux transformer [5] which provides an inductive coupling between the loops of the qubits. Depending on the details, $\hat\sigma_z^i \hat\sigma_z^j$, $\hat\sigma_z^i \hat\sigma_x^j$, or $\hat\sigma_x^i \hat\sigma_x^j$ couplings arise. This coupling can be turned on and off by a switch in the flux transformer. The related external circuit should be designed carefully to minimize decoherence effects.

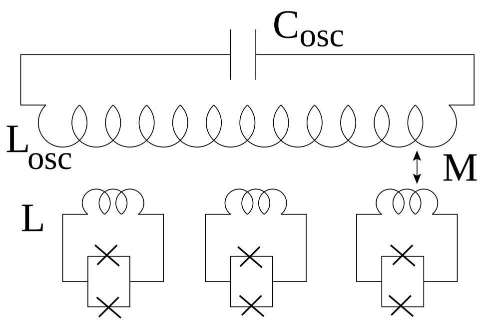

Figure 2. Coupling of flux qubits via an oscillator circuit.

Here we discuss another design of a many-qubit circuit, which allows one to control interactions without additional switches. The circuit, shown in Fig. 2, includes an LC-circuit formed by a loop with the self-inductance $L_{\rm osc}$, in series with a small capacitor $C_{\rm osc}$. The loop is coupled via a mutual inductance M to the set of flux qubits. After integrating out the oscillations which are assumed faster than the qubits' dynamics the effective coupling is found [1]:

$$\mathcal{H}_{\rm int} = -\pi^2 \left(\frac{M}{L}\right)^2 \sum_{i<j} \frac{\delta\Phi_i \delta\Phi_j}{\Phi_0^2} \frac{\Delta_i \Delta_j}{e^2/C_{\rm osc}} \; \hat{\sigma}_y^i \hat{\sigma}_y^j \; . \tag{3}$$

We note that the two-bit interaction can be controlled through the tunneling amplitudes Δ_i of the individual qubits. These can be switched off with exponential accuracy by increasing the barrier height $E_{\rm J}(\Phi'_{\rm x})$.

4. ENVIRONMENT AND DEPHASING

Due to the unavoidable coupling to environmental degrees of freedom the state of the qubits gets entangled with the environment, which leads to dephasing effects. Charge qubits are sensitive to electromagnetic fluctuations in the external circuit and in the substrate and to background charge fluctuations. Flux qubits are insensitive to the latter. Various sources of dissipation for flux qubits are discussed in Ref. [5]. Here we estimate the influence of the external circuit.

Control over the applied fluxes requires coupling the quantum system to a dissipative external circuit. This introduces fluctuation effects. Fluctuations in the circuit which controls the flux in the main loop of a flux qubit couple to the σ_z-degree of freedom. The external circuit can be parametrized by an effective impedance, which in turn can be modeled by an oscillator bath in the spirit of the Caldeira-Leggett model. The behavior of a two-state system coupled to an oscillator bath has been discussed in the context of the spin-boson model [12,13]. The results are that the decay of the off-diagonal elements of the density matrix of the qubit (dephasing) and the relaxation of the diagonal elements to their equilibrium values are described by the two time scales

$$\tau_\varphi = \gamma \; \frac{\hbar}{\Delta E} \; \left(\frac{1}{2} \coth \frac{\Delta E}{2k_{\rm B}T} \sin^2\eta + \frac{2k_{\rm B}T}{\Delta E} \cos^2\eta \right)^{-1} \; , \tag{4}$$

$$\tau_{\rm relax} = \gamma \; \frac{\hbar}{\Delta E} \; \left(\coth \frac{\Delta E}{2k_{\rm B}T} \sin^2\eta \right)^{-1} \; . \tag{5}$$

Here $\Delta E = \sqrt{\varepsilon^2 + \Delta^2}$ is the level spacing of the qubit, T the temperature, and $\eta \equiv \tan^{-1} \Delta/\varepsilon$.

The dimensionless parameter γ describes the strength of the dissipation. It is fixed by the impedance R_I (in units of $R_{\rm K} \equiv h/e^2$) of the current-source input circuit, providing the flux bias $\Phi_{\rm x}$, and its mutual inductance $M_{\rm in}$ with the qubit's loop:

$$\gamma = a \, \frac{R_I}{R_{\rm K}} \left(\frac{\Phi_0^2/4\pi^2 M_{\rm in}}{E_{\rm J}} \right)^2 \; . \tag{6}$$

The numerical prefactor is $a = \pi/6(\beta_L - 1)$ for the rf-SQUID and $a \sim 1$ for the design of Ref. [5]. The dephasing is slow for small loops and junctions with low critical currents.

Indeed, the argument in the bracket in (6) is proportional to $\beta_L^{-1} = \Phi_0^2/4\pi^2 L E_{\rm J}$. While $\beta_L^{-1} \le 1$ for the rf-SQUID, it can be much larger for the design of Mooij et al. [5], corresponding to slower dephasing.

The effect of fluctuations in the circuit providing the flux $\Phi_{\rm x}'$ (see Fig. 1b), which couple to the σ_x-term of the Hamiltonian, can be described in a similar way [2].

5. READ-OUT: QUANTUM MEASUREMENT

To measure the quantum state of a flux qubit, one needs a dissipative device sensitive to magnetic flux. Natural candidates are dc-SQUIDs, which have been used widely as ultra-sensitive magnetometers [14,15]. Coupling a dc-SQUID inductively to the qubit, as shown in Fig. 3a, makes its I–V characteristic sensitive to the qubit's state. For instance, a symmetric low-inductance dc-SQUID acts as a single Josephson junction with coupling energy controlled by the external flux, $E_{\rm J}(\Phi_{\rm x}) = 2E_{\rm J}^0 \cos(\pi\Phi_{\rm x}/\Phi_0)$. Here $E_{\rm J}^0$ is the Josephson energy of each of the two junctions in the loop. If this device is driven out of equilibrium by a current bias, the voltage response is sensitive to $E_{\rm J}(\Phi_{\rm x})$, and thus, to the state of the qubit.

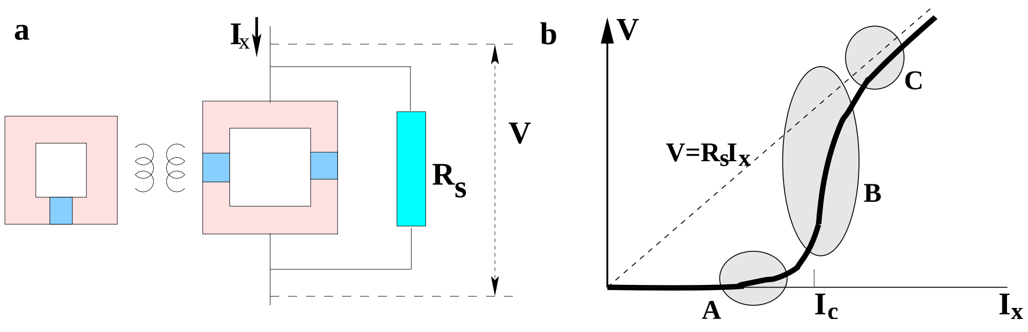

Figure 3. **a**. Measurement setup for a flux qubit. The rf-SQUID (qubit) is inductively coupled to the shunted dc-SQUID (meter). **b**. A schematic I–V characteristic of an overdamped dc-SQUID.

The physics of driven Josephson junctions is extremely rich; there are many regimes in which the measurements can be performed. Here we discuss the measurement of the switching current in hysteretic, underdamped SQUIDs, and the readout of the voltage response in overdamped SQUIDs biased above or below the critical current.

One proposed measurement strategy [5] is to use an underdamped dc-SQUID, without shunt or with high shunt resistance $R_{\rm s} > (1/2\pi\sqrt{2})\sqrt{E_{\rm C}/E_{\rm J}}\, R_{\rm K}$, where $E_{\rm J}$ and $E_{\rm C}$ are the characteristic Josephson and charging energies of the SQUID. The current-voltage characteristic of an underdamped SQUID is hysteretic. To read out the state of the qubit, the current in the SQUID is ramped from zero towards the critical value, and the value of current is recorded where the SQUID switches to the dissipative regime. As this switching current depends on the flux through the SQUID, information about the state of the qubit is obtained. Unfortunately, the current switching is a random process, fluctuating even when the external flux in the SQUID is fixed. For the systems studied in Ref. [10] this spread was larger than the difference in switching currents corresponding to the two states of the qubit. Therefore only statistical (weak) measurements were possible in this regime. Work is under way to improve the situation. The advantage of this strategy is that high shunt resistance R_s keeps the current noise at a low level. Therefore in the off-state, in spite of the permanent presence of the dc-SQUID, the coherent dynamics of the qubit suffers only weak dephasing.

Another strategy is to use an overdamped dc-SQUID with $R_\mathrm{s} < (1/2\pi\sqrt{2})\sqrt{E_\mathrm{C}/E_\mathrm{J}}\,R_\mathrm{K}$. Its I-V curve, sketched in Fig. 3b, is non-hysteretic. The highest sensitivity of the voltage response to the value of the critical current (and thus to the qubit's state) is reached at the current bias close to the critical value I_c, in the region B in Fig. 3b. On the other hand, a simple picture of the physics involved can be derived at I_x not too close to I_c, in the almost superconducting regime A and the dissipative regime C. In these regimes, as we describe below, the evolution reduces to a Poisson process of the phase (regime A) or charge (regime C) tunneling with a rate, which is sensitive to the qubit's state.

If $I_\mathrm{x} > I_\mathrm{c}$ (dissipative regime C), the current flows mostly through the shunt and the voltage drop across the dc-SQUID is close to $V_\mathrm{x} = I_\mathrm{x} R_\mathrm{s}$. However, the deviation of the voltage drop from V_x depends on I_c and carries the needed information. The description of the measurement process in terms of the time evolution of the phase drop ϕ introduces relevant time scales [16,6]. Here we present a description in terms of the charge variable. Indeed, the deviation of the voltage response from V_x is just $R_\mathrm{s} I_\mathrm{J}$, where $I_\mathrm{J} = I_\mathrm{x} - V/R_\mathrm{s}$ is the (small) fraction of the external current I_x that flows through the dc-SQUID. This current is carried by Cooper pairs which tunnel incoherently and dissipate their energy to the environment provided by the shunt. Concentration on the current I_J becomes even more natural in a circuit that is equivalent to that in Fig. 3a and consists of a voltage source V_x applied to the dc-SQUID and the shunt resistor R_s in series (Thévenin theorem). For this circuit the analysis is similar to that for the charge qubit measured by a normal SET, which has been described by an explicit analysis of the time evolution of the density matrix of the combined system of qubit and meter [17]. To keep track of the results of the measurement, we introduce a "counting" variable — the number m of electrons (in the case of a SET) or Cooper pairs (for a dc-SQUID) that have passed through the device since the start of the measurement. The evolution of this variable describes the current I_J and carries the needed information about the state of the qubit.

To show that this evolution is a Poisson process, let us consider first the Hamiltonian of the SQUID, $\mathcal{H} = 2eV_\mathrm{x} m - \frac{1}{2} E_\mathrm{J} \sum_m (|m\rangle\langle m+1| + \mathrm{h.c.})$. Its eigenenergies are equidistant, while the eigenstates $|\tilde{m}\rangle$ can span a wide range of charge states (of order $E_\mathrm{J}/V_\mathrm{x}$ at low voltages $V_\mathrm{x} < E_\mathrm{J}$) or be almost localized to a single charge state, $|\tilde{m}\rangle \approx |m\rangle$ (at higher $V_\mathrm{x} > E_\mathrm{J}$). In any case, the average charges in the eigenstates are also equidistant and differ by $2e$. Hence the motion along the staircase of the eigenstates is associated both with energy dissipation and charge transfer.

The voltage fluctuations δV induced by the bias circuit couple to the charge, $\mathcal{H}_\mathrm{int} = 2em\delta V$; their correlations being given by the Johnson-Nyquist form, $\langle \delta V_\omega^2 \rangle = \hbar\omega R_\mathrm{s}[1 + \coth(\hbar\omega/2k_\mathrm{B}T)]$. Due to its matrix structure in the eigenbasis, $\mathcal{H}_\mathrm{int}$ induces transitions only between the neighboring states, with the Golden rule rate $\Gamma = R_\mathrm{s} I_\mathrm{c}^2/4eV_\mathrm{x}$. Hence, the current $I_\mathrm{J} = 2e\Gamma$ and its noise are related: $S_{I_\mathrm{J}} = 4eI_\mathrm{J}$.

These results are in agreement with the derivation in Ref. [18] based on the Langevin equation for the phase variable ϕ. Notice that both the charge and the phase language can be used to describe the measurement process. This seems to contradict the uncertainty principle — the changes of two conjugate variables, charge $\int I_\mathrm{J} dt$ and phase $\int V dt$, are discussed in these two approaches. To resolve this paradox notice that the dynamics of the output signal (the voltage drop V on the junction or the current $I_\mathrm{J} = (V_\mathrm{x} - V)/R_\mathrm{s}$ through it) is only weakly sensitive to the initial values of charge and phase. Indeed, when the current bias $I_\mathrm{x} > I_\mathrm{c}$ is applied, the (initially well-defined) phase starts running down the washboard potential, but the time-averaged voltage $\int \dot\phi \; dt$ is not sensitive to the initial value of ϕ. As a consequence, one can read out the charge to obtain the needed information: this would smear the phase but would have no effect on the output signal. How the measurement of the current (i.e., m) would be performed in practice may be a complicated matter. However, it clearly can be done in principle, and this allows us to use the appealingly simple picture in the charge language to describe the readout process.

To illustrate the relation between the charge and phase pictures, one can derive the master equation for the reduced density matrix in the Wigner representation $\rho(\tilde m, \phi, t)$, where the integer $\tilde m$ enumerates the eigenstates. At low temperature, in the rotating-wave approximation and to first order in $R_\mathrm{s}/R_\mathrm{K}$ it reads:

$$\dot\rho(\tilde m, \phi, t) = \Gamma \left[\rho(\tilde m - 1, \phi, t) - \rho(\tilde m, \phi, t)\right] + \frac{2eV_\mathrm{x}}{\hbar} \frac{\partial}{\partial \phi} \rho(\tilde m, \phi, t) \; . \tag{7}$$

This equation describes the Poisson process of charge tunneling and, at the same time, the uniform shift of the phase variable. To describe the deviation of the voltage drop $\hbar\dot\phi/2e$ from V_x and the phase diffusion, one has to include higher-order terms.

Eq. (7) allows us to calculate the statistics of current, which is described by the probability distribution of the number of Cooper pairs m which have tunneled through the SQUID: $P(m,t)$. Due to the shot noise calculated above, the information about the qubit's state can be deduced from the current I_J only after a finite time, τ_meas. Indeed, at the start of the measurement no Cooper pairs have tunneled, and $P(m, t = 0) = \delta_{m0}$. Then the current starts flowing; the peak of $P(m,t)$ shifts in the direction of positive m and widens due to shot noise effects. Since the two flux states of the qubit correspond to different net currents, or different Cooper-pair tunneling rates $\Gamma_{1,2}$ through the SQUID, after some time the peak splits into two separated by $|\Gamma_1 - \Gamma_2|t$. The widths of the peaks grow as $\sqrt{\Gamma_{1,2} t}$ due to shot noise. Therefore the peaks are separated after time $\tau_\mathrm{meas} \approx (\sqrt{\Gamma_1} - \sqrt{\Gamma_2})^{-2}$. For the initial state of the qubit $a\,|0\rangle + b\,|1\rangle$ we find that after a time τ_meas a good quantum measurement is realized with weights of the peaks after the separation given by $|a|^2$ and $|b|^2$.

From the analysis of the time evolution of the density matrix we find that the evolution of the system during the measurement is characterized by three time scales. We have already introduced τ_meas, which describes the dynamics of the output signal, I_J. In addition the dynamics of the qubit's measurement is characterized by two more time scales. In the first stage, on a short time scale τ_φ, the nonequilibrium noise of the SQUID leads to the loss of phase coherence of the qubit, that is to the decay of the off-diagonal elements of the reduced 2×2 density matrix of the qubit. The coupling between the qubit and the SQUID may be written as $\mathcal{H}_{\rm int} = J\delta\Phi\sigma_z/2$, where J is the operator of the current circulating in the SQUID's loop and $\delta\Phi$ is the difference between the fluxes the qubit induces in the SQUID in its two states. In terms of these variables we find $1/\tau_\varphi \approx \delta\Phi^2\langle J^2_{\omega=0}\rangle/2$. As expected, the dephasing time cannot be longer than the measurement time, $\tau_\varphi \le \tau_{\rm meas}$. For a symmetric dc-SQUID at low temperature the equality is reached [16].

At long times, for finite Δ, the measurement induces transitions between the eigenstates of the qubit. After a "mixing time" $\tau_{\rm mix}$ the diagonal elements of the qubit's density matrix relax to 1/2, and the information about their initial values $|a|^2$, $|b|^2$ is lost. At this stage $P(m,t)$ develops a plateau between the two peaks and the weights of the peaks decay. At much longer times $t \gg \tau_{\rm mix}$ the plateau transforms into a single peak around $m = \bar\Gamma t$, where $\bar\Gamma \equiv (\Gamma_1 + \Gamma_2)/2$. The time evolution of $P(m,t)$ is depicted in Fig. 4. For convenience the probability distribution $p(m/t,t)$ of the quantity m/t, i.e., the Josephson current averaged over time t, is shown.

While for the time-resolved measurements information about the qubit's state gets lost at long times, the stationary-state noise characteristics of the combined system of qubit and meter still provides information about the relevant time scales τ_φ, $\tau_{\rm meas}$, $\tau_{\rm mix}$ [16,19].

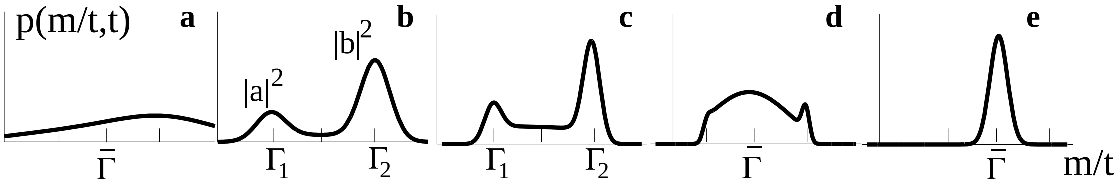

Figure 4. The evolution of the probability distribution $p(m/t,t)$ for the values of the average current in the SQUID. The initial state of the qubit is $a|0\rangle + b|1\rangle$ with $a = 1/2$, $b = \sqrt{3}/2$. **a**. $t < \tau_{\rm meas}$: a very broad peak due to shot noise. **b**. $\tau_{\rm meas} < t < \tau_{\rm mix}$: two peaks separate. **c**–**e**. $t \sim \tau_{\rm mix}$ and $t > \tau_{\rm mix}$: a plateau grows between the two peaks, erasing the information about the initial state of the qubit.

Finally, we turn to a dc-SQUID biased below the critical current, $I_{\rm x} < I_{\rm c}$ (regime A). The voltage response is weak since most of the current flows trough the SQUID as a supercurrent. In terms of the phase drop ϕ across the junction, the system spends most of the time in a minimum of the washboard potential, $-E_{\rm J}(\Phi_{\rm x})\cos\phi - I_{\rm x}\phi$. The dynamics of the phase is due to tunneling events to neighboring minima. The quantum-tunneling or thermal transition rate of single flux quanta determines the voltage response, and the dynamics in this regime is Poissonian. The measurement can again be described by a probability distribution $P(m,t)$ with similar properties as described above, where m is now the number of flux quanta which have passed across the dc-SQUID. Notice that the tunneling is exponentially suppressed at $I_{\rm x} \ll I_{\rm c}$ but becomes observable closer to $I_{\rm c}$. On the other hand, the relative sensitivity of the voltage drop to the qubit's state is exponentially high in this regime.

6. DEPHASING IN THE OFF-STATE

One of the reasons why underdamped SQUIDs are considered to be suitable meters is their low noise level in the off-state. Here we point out that also for overdamped SQUIDs the dephasing of the qubit in the off-state can be suppressed by a proper choice of parameters.

For the symmetric SQUID in Fig. 3a the qubit-detector interaction, $-E_{\rm J}(\Phi+\delta\Phi\ \hat{\sigma}_z/2)\cos\varphi$, may be approximated in the off-state as $\delta E_{\rm J}\ \hat{\sigma}_z\ \varphi^2/4$, where $\delta E_{\rm J} = [\partial E_{\rm J}(\Phi)/\partial\Phi]\delta\Phi$. This interaction is quadratic rather then linear in φ. On the other hand, as the phase φ is directly coupled to the oscillator bath of the shunt resistor. We thus arrive at the following Hamiltonian

$$\begin{aligned}\mathcal{H} &= \frac{1}{2}\varepsilon\ \hat{\sigma}_z + \frac{1}{2}\Delta\ \hat{\sigma}_x + \frac{q^2}{2C} + \frac{1}{2}E_{\rm J}(\Phi)\ \varphi^2 + \sum_i \left(\frac{p_i^2}{2m_i} + \frac{m_i\omega_i^2 x_i^2}{2}\right) \\ &+ \frac{1}{4}\delta E_{\rm J}\ \hat{\sigma}_z\ \varphi^2 + \varphi\sum_i \lambda_i x_i\ .\end{aligned} \tag{8}$$

The phase φ interacts linearly with the bath, while the qubit is coupled to φ^2. The shunt resistor is represented by oscillators x_i, p_i with Ohmic spectral density

$$J(\omega) \equiv \frac{\pi}{2}\sum_i \frac{\lambda_i^2}{m_i\omega_i}\ \delta(\omega-\omega_i) = \frac{R_K}{R}\omega\ . \tag{9}$$

Using a short time expansion we estimate the dephasing rate as

$$(\tau_\varphi^{\rm off})^{-1} = \left(\frac{\delta E_{\rm J}}{2\hbar}\right)^2 \int \frac{d\omega}{2\pi}\left\langle\varphi_\omega^2\right\rangle\left\langle\varphi_{-\omega}^2\right\rangle\ , \tag{10}$$

where

$$\left\langle\varphi_\omega^2\right\rangle = \frac{2\pi}{\omega}\frac{{\rm Re}Z(\omega)}{R_{\rm K}}\left(\coth\frac{\omega}{2T}+1\right)\ , \qquad Z(\omega) = \left(\frac{1}{R} + i\omega C + \frac{2\pi I_c}{i\omega\Phi_0}\right)^{-1}\ . \tag{11}$$

From this we obtain

$$\tau_\varphi^{\rm off} = \frac{eI_c}{(I_{c,\uparrow}-I_{c,\downarrow})^2}\begin{cases} (12/\pi^2)\ (8\pi E_{\rm J}/T)^3\ (R/R_{\rm K})^2, & T \ll (4R/R_{\rm K})E_{\rm J}, \\ (16/\pi)\ (8\pi E_{\rm J}/T)^2\ \ R/R_{\rm K}\ \ , & T \gg (4R/R_{\rm K})E_{\rm J}, \end{cases} \tag{12}$$

where $I_{c,\uparrow}$ and $I_{c,\downarrow}$ are the values of the critical current corresponding to the two states of the qubit. Thus we observe that, even in the overdamped regime with low R, the dephasing may be slow at low enough temperatures. In contrast to the spin-boson case, the dephasing rate scales as T^3.

7. SUMMARY

First qubits based on the flux degree of freedom have been fabricated and the experiments demonstrated quantum-mechanical effects of the macroscopic phase (flux) variable. A further step would be an observation of macroscopic quantum coherence, i.e., of coherent oscillations of the flux between two macroscopically different values. To achieve this goal, further reductions of dephasing effects are necessary. While phase qubits are less sensitive to the background charge fluctuations, the major source of dephasing for charge qubits, they may couple stronger to the magnetic noise. This strong dephasing may have hindered the observation of coherent flux oscillations in recent experiments. Furthermore, the readout devices should be optimized to diminish the noise in the off-state. Our analysis shows that a compromise between overdamped and underdamped regimes of the SQUID dynamics may have to be considered. The potentially strong dephasing of the qubit by an overdamped SQUID may be strongly suppressed by cooling the system down.

Our description of the measurement process shows an interesting interplay between the charge and phase dynamics. These effects should be investigated further and one may think of combining advantages of phase and charge qubits and detectors to optimize the properties of the device. This may require coupling together of charge and flux qubits or going over into an intermediate regime.

Acknowledgments

The work is part of the CFN (Center for Functional Nanostructures) which is supported by the DFG (German Science Foundation). Y.M. is supported by the Humboldt Foundation, BMBF and the programme ZIP of the German government.

REFERENCES

1. A. Shnirman, G. Schön, Z. Hermon, Phys. Rev. Lett. **79** (1997) 2371.
2. Yu. Makhlin, G. Schön, A. Shnirman, Nature **386** (1999) 305.
3. D. V. Averin, Solid State Commun. **105** (1998) 659.
4. L. B. Ioffe et al., Nature **398** (1999) 679.
5. J. E. Mooij et al., Science **285** (1999) 1036.
6. Yu. Makhlin, G. Schön, A. Shnirman, Rev. Mod. Phys. **73** (2001) 357.
7. A. J. Leggett, in: *Chance and Matter*, J. Souletie, J. Vannimenus, R. Stora (Eds.), Elsevier, Amsterdam, 1987, p. 395.
8. C. D. Tesche, Phys. Rev. Lett. **64** (1990) 2358.
9. T. P. Orlando et al., Phys. Rev. B **60** (1999) 15398.
10. C. H. van der Wal et al., Science **290** (2000) 773.
11. J. R. Friedman et al., Nature **406** (2000) 43.
12. A. J. Leggett et al., Rev. Mod. Phys. **59** (1987) 1.
13. U. Weiss, *Quantum dissipative systems*, World Scientific, Singapore, 1999.
14. M. Tinkham, *Introduction to superconductivity*, McGraw-Hill, New York, 1996.
15. K. K. Likharev, *Dynamics of Josephson junctions and circuits*, Gordon and Breach, Amsterdam, 1996.
16. D. V. Averin, e-print cond-mat/0004364 .
17. A. Shnirman, G. Schön, Phys. Rev. B **57** (1998) 15400.
18. R. H. Koch, D. J. Van Harlingen, J. Clarke, Phys. Rev. Lett. **45** (1980) 2132.
19. Yu. Makhlin, G. Schön, A. Shnirman, Phys. Rev. Lett. **85** (2000) 4578.